ULTRASOUND NEWS

Mars-2025

Cureus

Open Access Original Article

Surgeon-Performed Point-of-Care Ultrasound in the Diagnosis of Acute Sigmoid Diverticulitis: A Pragmatic Prospective Multicenter Cohort Study

Abstract

Background and purpose

Aims

Patients and methods

Results

Conclusion

bowel wall thickness ≥ 4mm, pain on graded compression, pericolic fat changes (increased echogenicity), and diverticula

abscess, fistula, the presence of free fluid and the absence of peristalsis defined complicated diverticulitis

.

Modified Hinchey Classification	
Class	CT findings
Stage 0	Mild clinical diverticulitis
Stage Ia	Confined pericolic inflammation
Stage Ib	Confined pericolic abscess (<5cm) from the inflammatory site
Stage II	Diverticulitis with abscess distant from the primary inflammatory site (intra-abdominal, retroperitoneal, or pelvic)
Stage III	Generalized purulent peritonitis
Stage IV	Generalized fecal peritonitis

Khoa : **SIÊU ÂM TỔNG QUÁT** - Phòng 22
Máy: **ALOKA -ProSound SSD4000**

KẾT QUẢ SIÊU ÂM MÀU

ID : **7994974** Ngày ĐK: 10/01/2025 06:18
Họ và tên : **35** tuổi **Nam**
Địa chỉ :
Chẩn đoán sơ bộ : ĐAU ÂM Ỉ BỤNG PHẢI 2 NGÀY. TC: RL PHÂN 1 THÁNG.
BS chỉ định : BS. CKII. NGUYỄN VĂN HIỀN BV chỉ định : MEDIC

VÙNG KHẢO SÁT : SIÊU ÂM BỤNG TỔNG QUÁT MÀU

- GAN: Không to, bờ đều, cấu trúc đồng dạng, không sang thương khu trú.
- TÚI MẬT: không sỏi, vách mỏng. Đường mật trong gan không dãn. Ống mật chủ không sỏi, không dãn.
- TỤY: bình thường. LÁCH: Không to, đồng dạng.
- THẬN P: không sỏi, không ứ nước.
- THẬN T: không sỏi, không ứ nước.

Hai thận cấu trúc và kích thước bình thường, giới hạn vỏ - tủy rõ.

- BÀNG QUANG: không sỏi, vách mỏng.
- TIỀN LIỆT TUYẾN: không to.
- Động mạch chủ bụng không phình. Ascites (-). Không hạch ổ bụng. Cocard sign (-). Không tràn dịch màng phổi.
- HỐ CHẬU PHẢI: có ít dịch tự do, d=10mm. Chưa thấy ruột thừa viêm.
- CẠNH NGOÀI ĐẠI TRÀNG PHẢI: có vài túi thừa viêm, d=8-20mm, mạc nối xung quanh phù nề, d # 54x27mm, không tụ dịch.

KẾT LUẬN : - VIÊM TÚI THỪA ĐẠI TRÀNG PHẢI.
- ÍT DỊCH TỰ DO VÙNG HỐ CHẬU PHẢI.

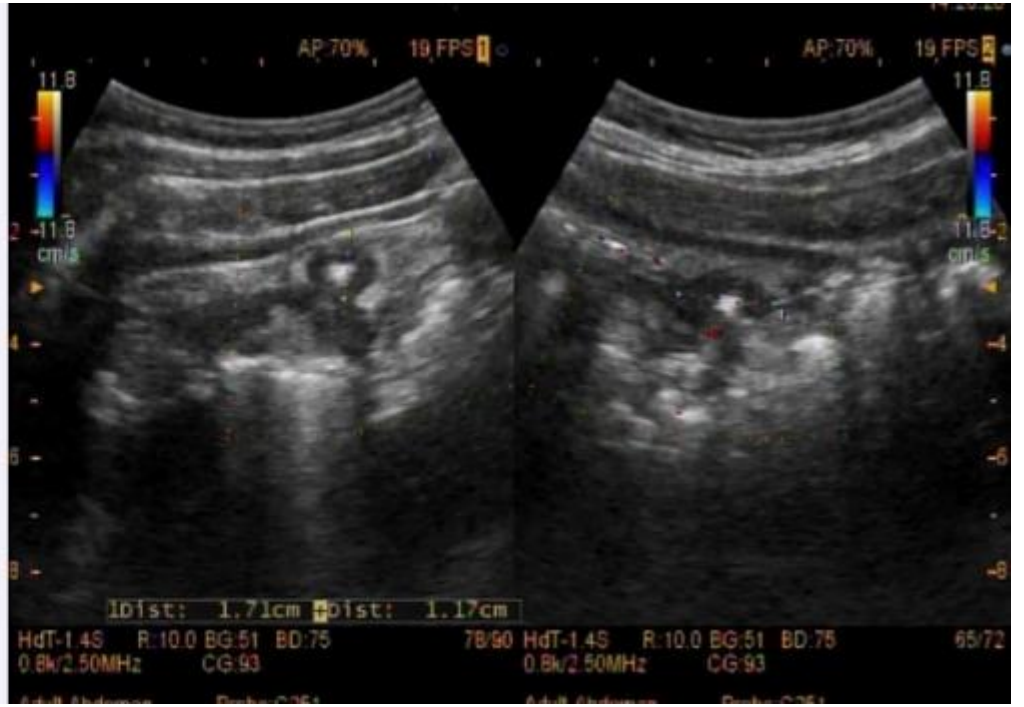

Thrombus stiffness as an independent predictor of endovascular treatment success in hemodialysis fistulas: a study using ultrasound elastography

Sarhun Zirek[1], Gökhan Mert Özyurt[1], Alptuğ Özen[1], Refik Olmaz[2], Kaan Esen[3]

[1]Department of Radiology, Mersin City Training and Research Hospital, Mersin; [2]Department of Nephrology, Mersin City Training and Research Hospital, Mersin; [3]Department of Radiology, Mersin University Faculty of Medicine Research and Application Hospital, Mersin, Turkey

ULTRA SONO GRAPHY

ORIGINAL ARTICLE

https://doi.org/10.14366/usg.24175
eISSN: 2288-5943
Ultrasonography 2025;44:153-159

Purpose: This study aimed to evaluate the prognostic value of thrombus stiffness, measured by strain elastography, in independently predicting the success of endovascular treatment for thrombosed hemodialysis fistulas.

Methods: The study employed a retrospective observational design. Forty-nine patients with chronic kidney disease undergoing hemodialysis and experiencing fistula dysfunction were included. Various factors were evaluated, including patient age, sex, comorbidities, arteriovenous fistula (AVF) type, use of antiplatelet agents, duration of thrombosed AVF dysfunction, thrombus length, thrombus stiffness, and thrombus strain ratio (SR). Thrombus stiffness was measured using strain ultrasound elastography.

Results: The presence of comorbidities (P=0.018), duration of AVF dysfunction due to thrombosis (P=0.005), thrombus stiffness (P<0.001), and thrombus SR (P<0.001) were statistically significant predictors of treatment success, while other factors were not. Thrombus stiffness and SR, assessed by two independent radiologists with excellent inter-reader agreement, demonstrated high reliability. The optimal SR cut-off for treatment success was 1.4 (sensitivity, 0.947; specificity, 0.901; area under the curve, 0.935). Multivariable logistic regression analysis revealed that both thrombus SR and thrombus stiffness significantly influenced treatment outcomes (P=0.003 and P=0.007, respectively). A 0.1-unit increase in thrombus SR was associated with 9.37% reduction in the likelihood of treatment success, while a smilar increase in thrombus stiffness exhibited an 8.06% reduction, underscoring their importance as prognostic factors in clinical setting.

Conclusion: This study demonstrates the utility of strain ultrasound elastography in assessing thrombus stiffness in thrombosed hemodialysis AVFs and its correlation with treatment success.

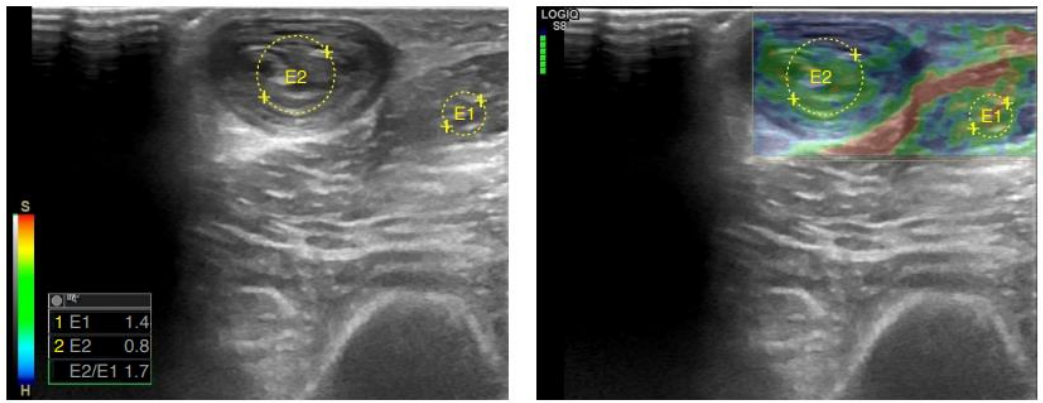

A B

Fig. 1. Strain elastography (A) and elastography map (B) images of a patient with hemodialysis arteriovenous fistula dysfunction due to thrombosis.
The surrounding soft tissue is identified as the reference point and marked with the E1 region of interest (ROI) circle. The thrombus within the vascular lumen was identified with the E2 ROI circle, and the ratio to the reference tissue (E1) was calculated by the device using the formula strain ratio=E2/E1. In this shared case, the strain ratio was calculated as 1.7, and the endovascular treatment performed was unsuccessful.

Novel non-invasive and quantitative assessment of the renal function of transplanted kidneys using Doppler ultrasonography with the vascular index of superb microvascular imaging

Sung Hwan Bae, Eun Ji Lee, Jiyoung Hwang, Seong Sook Hong, Yun-Woo Chang, Boda Nam

Department of Radiology, Soonchunhyang University Seoul Hospital, Soonchunhyang University College of Medicine, Seoul, Korea

Purpose: This study assessed the reproducibility and clinical value of the vascular index (VI), derived from superb microvascular imaging (SMI) using Doppler ultrasonography, for evaluating renal function in transplanted kidneys.

Methods: This retrospective study included 63 renal transplant patients who underwent grayscale and Doppler ultrasonography with SMI from January 2022 to February 2023. The VI of the transplanted kidneys was measured using three methods (VI_{box}, VI_{F1}, VI_{F2}). The VI was compared across chronic kidney disease (CKD) groups categorized by estimated glomerular filtration rate (eGFR) and Kidney Disease: Improving Global Outcomes (KDIGO) CKD risk groups based on eGFR and albuminuria. The correlation between VI and renal function was evaluated. Univariate and multivariate linear regression analyses were used to identify predictors of eGFR.

Results: Significant differences in VI were observed among CKD groups based on eGFR (VI_{box}, P=0.001; VI_{F1}, P<0.001; VI_{F2}, P<0.001) and KDIGO CKD groups based on eGFR and albuminuria (VI_{box}, P=0.039; VI_{F1}, P=0.001; VI_{F2}, P<0.001). VI_{F1} and VI_{F2} demonstrated moderate/high correlations with eGFR (r=0.627, P<0.001 and r=0.657, P<0.001, respectively) and serum creatinine (r=−0.626, P<0.001 and r=−0.649, P<0.001, respectively). VI_{box} moderately correlated with eGFR (r=0.445, P<0.001). Multivariate regression identified the urine albumin-creatinine ratio (ACR) (adjusted odds ratio [aOR], 1.122; 95% confidence interval [CI], −0.007 to, 0.000; P=0.030) and VI_{F2} (aOR, 1.114; 95% CI, 0.466 to 1.235; P<0.001) were independently associated with eGFR.

Conclusion: The VI measured by drawing a region of interest along the border of the transplanted kidney in SMI (VI_{F2}) is highly reproducible and correlates well with eGFR. Both VI_{F2} and ACR independently predict eGFR.

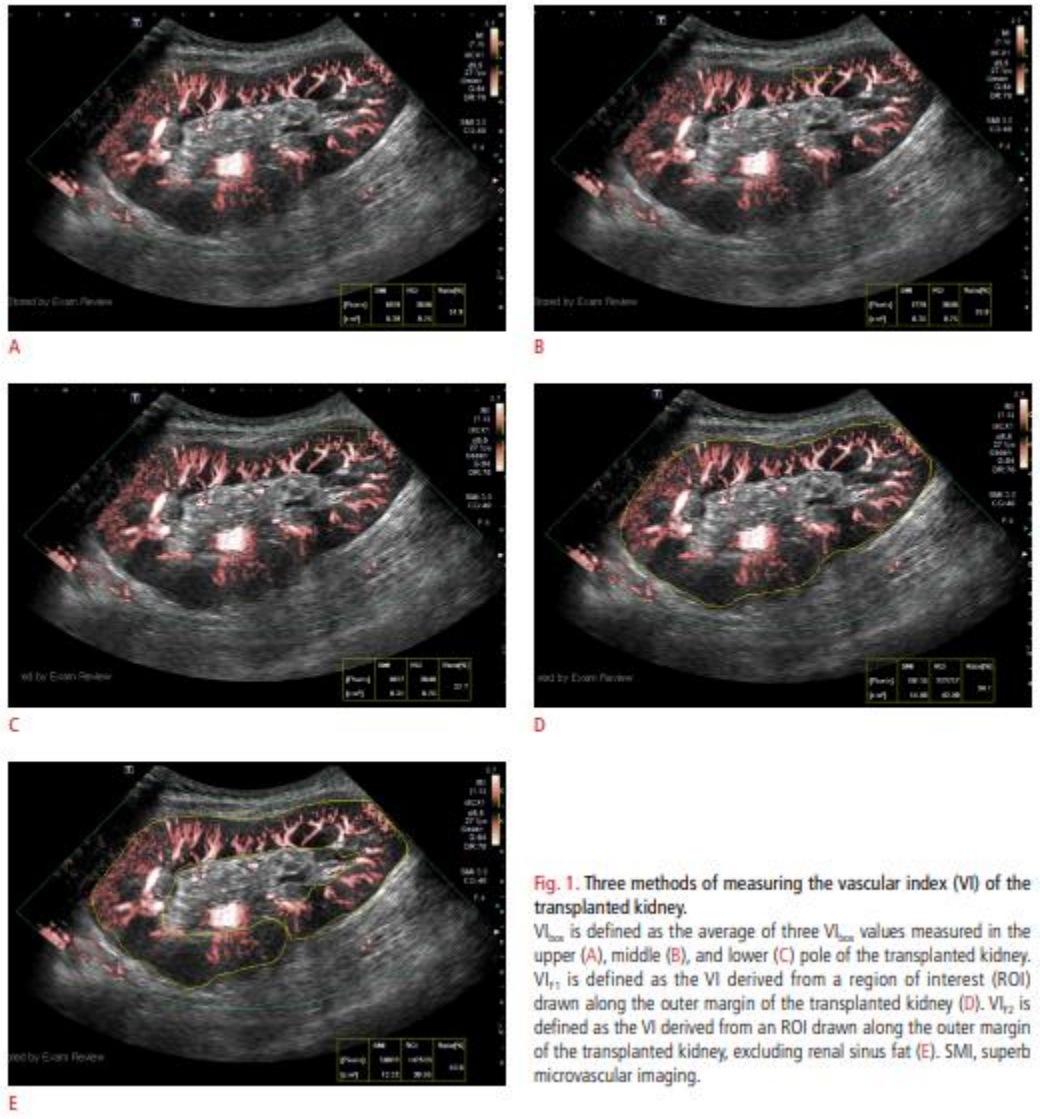

Fig. 1. Three methods of measuring the vascular index (VI) of the transplanted kidney.
VI_{box} is defined as the average of three VI_{box} values measured in the upper (A), middle (B), and lower (C) pole of the transplanted kidney. VI_{F1} is defined as the VI derived from a region of interest (ROI) drawn along the outer margin of the transplanted kidney (D). VI_{F2} is defined as the VI derived from an ROI drawn along the outer margin of the transplanted kidney, excluding renal sinus fat (E). SMI, superb microvascular imaging.

The VI measured by drawing a region of interest along the border of the transplanted kidney in SMI (VI_{F2}) is highly reproducible and correlates well with eGFR. Both VI_{F2} and ACR independently predict eGFR.

Ultrasound-guided attenuation parameter for identifying metabolic dysfunction–associated steatotic liver disease: a prospective study

Yun-Lin Huang[1]*, Chao Sun[2]*, Ying Wang[3], Juan Cheng[3], Shi-Wen Wang[3], Li Wei[3], Xiu-Yun Lu[3], Rui Cheng[3], Ming Wang[3], Jian-Gao Fan[2], Yi Dong[1,3]

[1]Department of Ultrasound, Zhongshan Hospital Fudan University, Shanghai; [2]Center for Fatty Liver Disease, Department of Gastroenterology, Xinhua Hospital Affiliated to Shanghai Jiao Tong University School of Medicine, Shanghai Key Lab of Pediatric Gastroenterology and Nutrition, Shanghai; [3]Department of Ultrasound, Xinhua Hospital Affiliated to Shanghai Jiao Tong University School of Medicine, Shanghai, China

Purpose: This study assessed the performance of the ultrasound-guided attenuation parameter (UGAP) in diagnosing and grading hepatic steatosis in patients with metabolic dysfunction–associated steatotic liver disease (MASLD). Magnetic resonance imaging proton density fat fraction (MRI-PDFF) served as the reference standard.

Methods: Patients with hepatic steatosis were enrolled in this prospective study and underwent UGAP measurements. MRI-PDFF values of ≥5%, ≥15%, and ≥25% were used as references for the diagnosis of steatosis grades ≥S1, ≥S2, and S3, respectively. Spearman correlation coefficients and area under the receiver operating characteristic curves (AUCs) were calculated.

Results: Between July 2023 and June 2024, the study included 88 patients (median age, 40 years; interquartile range [IQR], 36 to 46 years), of whom 54.5% (48/88) were men and 45.5% (40/88) were women. Steatosis grades exhibited the following distribution: 22.7% (20/88) had S0, 50.0% (44/88) had S1, 21.6% (19/88) had S2, and 5.7% (5/88) had S3. The success rate for UGAP measurements was 100%. The median UGAP value was 0.74 dB/cm/MHz (IQR, 0.65 to 0.82 dB/cm/MHz), and UGAP values were positively correlated with MRI-PDFF (r=0.77, P<0.001). The AUCs of UGAP for the diagnoses of ≥S1, ≥S2, and S3 steatosis were 0.91, 0.90, and 0.88, respectively. In the subgroup analysis, 98.4% (60/61) of patients had valid controlled attenuation parameter (CAP) values. UGAP measurements were positively correlated with CAP values (r=0.65, P<0.001).

Conclusion: Using MRI-PDFF as the reference standard, UGAP demonstrates good diagnostic performance in the detection and grading of hepatic steatosis in patients with MASLD.

ULTRA SONO GRAPHY

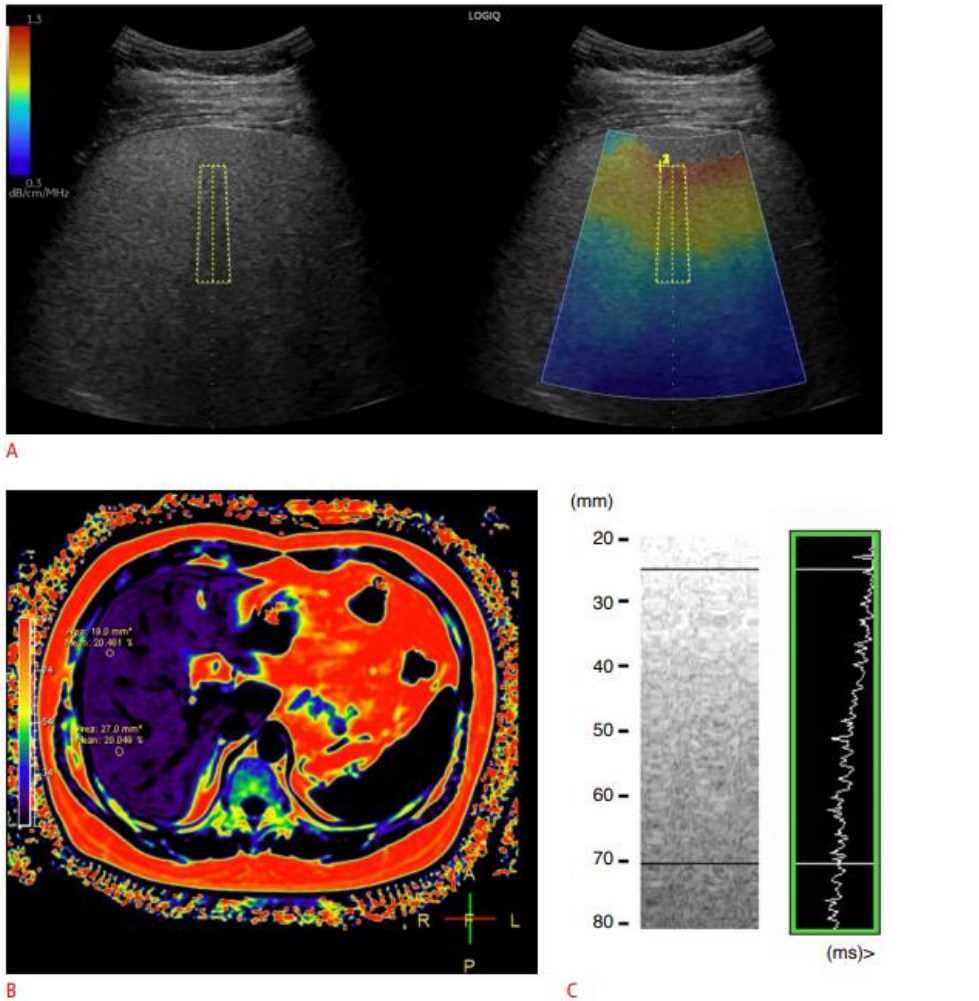

Fig. 6. A 34-year-old woman with metabolic dysfunction–associated steatotic liver disease and a body mass index of 31.2 kg/m^2. A. The ultrasound-guided attenuation parameter image displays a value of 0.82 dB/cm/MHz. B. The magnetic resonance imaging proton density fat fraction image indicates a mean value of 20.0%. C. The controlled attenuation parameter image closest to the reported value was selected as representative, with a value of 333 dB/m.

Ultrasound Attenuation, Liver Texture Index, and HepatoRenal Index: Assessing Reproducibility and Inter-operator Consistency in Clinical Practice

Fan Liu[1,2], Haiyan Zeng[2], Xingxing Yuan[2], Lingyue Du[2], Xiaoting Wu[2], Xue Han[2], Zaiqiang Chen[3], Shuai Yang[4], Jian Zheng[1,2]

[1]The First School of Clinical Medicine, Guangdong Medical University, Zhanjiang, [2]Ultrasound Department of The Second Affiliated Hospital, School of Medicine, The Chinese University of Hong Kong, Shenzhen and Longgang District People's Hospital of Shenzhen, Shenzhen, [3]Health Education Department of The Second Affiliated Hospital, School of Medicine, The Chinese University of Hong Kong, Shenzhen and Longgang District People's Hospital of Shenzhen, Shenzhen,[4] Department of Clinical and Research, Shenzhen Mindray Bio-medical Electronics Co., Ltd., Shenzhen, China

Abstract

Aim: This study aimed to evaluate the reproducibility of Ultrasound Attenuation (USAT), the Liver Texture Index (LTI) and the HepatoRenal Index (HRI). **Material and methods:** Between May 2023 to December 2023, 279 patients who underwent USAT, LTI and HRI tests at the Ultrasound Department of The Second Affiliated Hospital, School of Medicine, The Chinese University of Hong Kong, Shenzhen were included. All patients were examined by a physician with over 4 years of ultrasound experience. The intra-class correlation coefficient (ICC) was utilized to assess the reproducibility of the three quantitative parameters in all patients. Additionally, 63 cases were examined by another physician with six months of experience to evaluate inter-operator reproducibility. **Results:** The intra-operator reproducibility of USAT, LTI, and HRI were 0.879 (95% CI:0.858-0.898), 0.919 (95% CI:0.904-0.933), and 0.836 (95% CI:0.809-0.862), respectively. The inter-operator reproducibility among different operators were 0.790 (95% CI:0.604-0.894), 0.782 (95% CI:0.591-0.890), and 0.631 (95% CI:0.356-0.806). After 30 operations, the inter-operator reproducibility improved to 0.858 (95% CI:0.731-0.927), 0.909 (95% CI:0.823-0.954), and 0.796 (95% CI:0.587-0.899). **Conclusions:** USAT, LTI, and HRI have shown good intra-operator reproducibility, and inter-operator reproducibility between the two operators reached a comparable level after 30 training cases.

Keywords: UltraSound Attention (USAT); Liver Texture Index (LTI); HepatoRenal Index (HRI); Hepatic Steatosis; Reproducibility

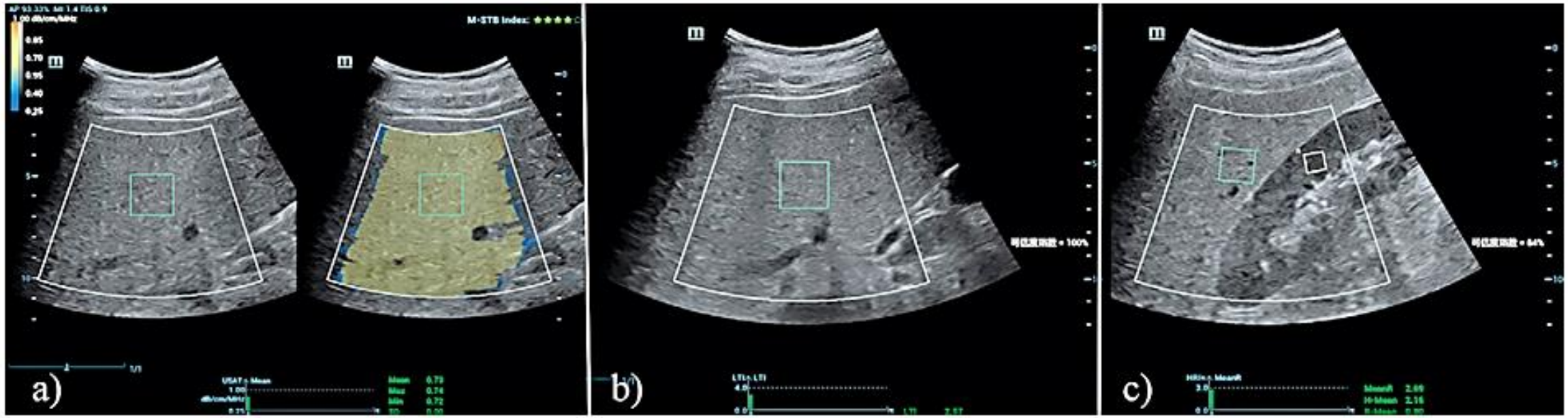

Fig 2. Measured images of ultrasound attention, liver texture index, and hepatorenal index in the same patient with fatty liver disease: a) ultrasound attention; b) liver texture inde; c) hepatorenal index

Ultrasound Attenuation (USAT): The right hepatic parenchyma was selected to avoid rib shadows, with the region of interest (ROI) avoiding large blood vessels where possible. The upper edge of the ROI was positioned approximately 1-2 cm away from the hepatic capsule, as close to the center of the image as feasible. The probe was perpendicular to the hepatic capsule, and the patient was instructed to hold their breath in a calm respiratory state. The image was then stabilized, frozen, and measurements were taken (fig 2a).

Liver Texture Index (LTI): The right liver parenchy ma was chosen to avoid rib shadows, with the ROI positioned to avoid large blood vessels. The ROI was placed Med Ultrason 2025; 0: 1-7 3 Fig 2. Measured images of ultrasound attention, liver texture index, and hepatorenal index in the same patient with fatty liver dis ease:

a) ultrasound attention;
b) b) liver texture index;
c) hepatorenal index as close to the center of the image as possible. The probe was perpendicular to the hepatic capsule, and the patient was instructed to hold their breath in a calm respiratory state. The image was frozen and measurements were taken once the image had stabilized (fig 2b).

HepatoRenal Index (HRI): A longitudinal section of the liver and right kidney was selected to avoid rib shad ows, with the ROI avoiding large blood vessels as much as possible. A large green box was placed in the liver pa renchyma, and a small yellow box in the renal cortex. The patient was instructed to hold their breath in a calm respiratory state. The image was then frozen and meas urements were taken after stabilization (fig 2c).

Improving breast ultrasonography education: the impact of AI-based decision support on the performance of non-specialist medical professionals

Sangwon Lee[1], Hye Sun Lee[2], Eunju Lee[2], Won Hwa Kim[3,4], Jaeil Kim[4,5], Jung Hyun Yoon[1]

[1]Department of Radiology, Severance Hospital, Research Institute of Radiological Science, Yonsei University College of Medicine, Seoul; [2]Biostatistics Collaboration Unit, Yonsei University College of Medicine, Seoul; [3]Department of Radiology, School of Medicine, Kyungpook National University, Kyungpook National University Chilgok Hospital, Daegu; [4]BeamWorks Inc., Daegu; [5]School of Computer Science and Engineering, Kyungpook National University, Daegu, Korea

Purpose: This study evaluated the educational impact of an artificial intelligence (AI)–based decision support system for breast ultrasonography (US) on medical professionals not specialized in breast imaging.

Methods: In this multi-case, multi-reader study, educational materials, including American College of Radiology Breast Imaging Reporting and Data System (BI-RADS) descriptors, were provided alongside corresponding AI results during training. The AI system presented results in the form of AI-heatmaps, AI scores, and AI-provided BI-RADS assessment categories. Forty-two readers evaluated the test set in three sessions: the first session (S1) occurred before the educational intervention, the second session (S2) followed education without AI assistance, and the third session (S3) took place after education with AI assistance. The area under the receiver operating characteristic curve (AUC), sensitivity, specificity, and overall performance, were compared between the sessions.

Results: The mean sensitivity increased from 66.5% (95% confidence interval [CI], 59.2% to 73.7%) to 88.7% (95% CI, 84.1% to 93.3%), with a statistically significant difference (P<0.001), and the AUC non-significantly increased from 0.664 (95% CI, 0.606 to 0.723) to 0.684 (95% CI, 0.620 to 0.748) (P=0.300). Both measures were higher in S2 than in S1. The AI-achieved AUC was comparable to that of the expert reader (0.747 [95% CI, 0.640 to 0.855] vs. 0.803 [95% CI, 0.706 to 0.900], P=0.217). Additionally, with AI assistance, the mean AUC for inexperienced readers was not significantly different from that of the expert reader (0.745 [95% CI, 0.660 to 0.830] vs. 0.803 [95% CI, 0.706 to 0.900], P=0.120).

Conclusion: The mean AUC and sensitivity improved after incorporating AI into breast US education and interpretation. AI systems with high-level performance for breast US can potentially be used as educational tools in the interpretation of breast US images.

Keywords: Breast; Ultrasound; Breast neoplasms; Artificial intelligence; Education

Key points: The diagnostic performance of non-specialist medical professionals improved following artificial intelligence (AI)–based education on breast ultrasound, with mean sensitivity increasing from 66.5% to 88.7% (P<0.001). With AI assistance, the mean area under the receiver operating characteristic curve for inexperienced readers was not significantly different from that of the expert reader following education; 0.745 (95% confidence interval [CI], 0.660 to 0.830) versus 0.803 (95% CI, 0.706 to 0.900), respectively (P=0.120). An AI system can be an educational tool for less experienced readers.

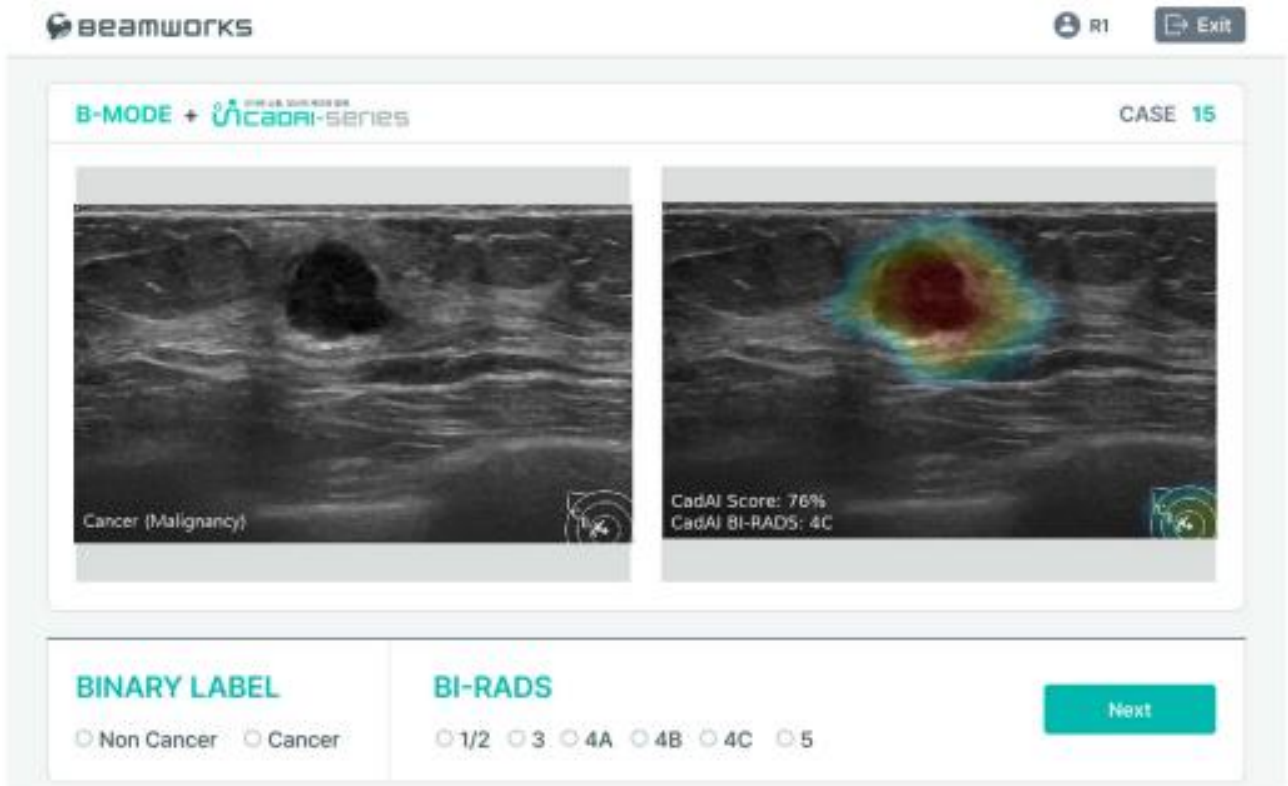

Fig. 1. Image of a display presented by the web-based system for image review in Session 3. A grayscale ultrasonography is on the left. Artificial intelligence (AI) analysis results are simultaneously displayed on the right, with a semi-transparent colored heatmap, AI score, and AI-provided Breast Imaging Reporting and Data System (BI-RADS) final assessment shown in the bottom corner. Participants were asked to mark their interpretations according to (1) binary scale (non-cancer vs. cancer), and (2) BI-RADS final assessment with subcategorizations for BI-RADS 4.